Non-destructive Inspection of Electro-Mechanical Systems using Micro X-ray Computed Tomography
(Proposal of CT reconstruction methods for eliminating metal artifacts)

Michihiko KOSEKI, Shuhei HASHIMOTO, Shinpei SATO, Hitoshi KIMURA and Norio INOU
Department of Mechanical and Control Engineering, Tokyo Institute of Technology
2-12-1, O-okayama, Meguro-ku, Tokyo, 152-8550 JAPAN
koseki@mech.titech.ac.jp

Abstract

Micro computed tomography (μCT) is quite useful for quality evaluation of electro-mechanical systems because it provides three-dimensional geometrical information of internal structures. However, large differences in x-ray absorption coefficients of materials produce metal artifacts in the CT images. This study aims to develop a new reconstruction algorithm to reduce the artifacts from the images and establish a non-destructive inspection technique of electro-mechanical systems using x-ray CT imaging. This paper discusses the cause of the artifacts and proposes two algorithms to reduce them. One is direct signal conversion technique of the projection data, and the other uses two projection data based on different x-ray intensities. We apply the methods to several samples and discuss the efficiency of the methods.

1. Introduction

Recent electro-mechanical systems, including MEMS devices, have been composed of various materials, such as metals, resins or carbon fibers. Commercial values of these systems depend on not only machining accuracy of each part but also assembly accuracy of the whole systems. For quality evaluation of the systems, Micro computed tomography (μCT) has a potential to become a great efficient device because it provides three-dimensional geometrical information of internal structures. However, large differences in x-ray absorption coefficients of materials sometimes produce artifacts with streak and star pattern in the CT images. The artifact, which is generally called "metal artifact," makes it difficult to discriminate materials in the device. Consider a lens unit of a digital camera for example. The unit is composed of multiple materials, such as resins, glasses, metals, ceramics, and so on. There are some inspection items for the unit such as thermal or structural damage after fatigue testing. In these inspections, it is inevitable to evaluate conditions of resin parts in the device, however the metal artifacts in the CT image disturb detail observation of the resin part. Therefore, new CT reconstruction algorithm which produces precise images without metal artifacts is strongly required in the production fields to realize non-destructive inspection technique for the assembly accuracy of the devices.

There have been several reconstruction techniques which reduce metal artifacts from CT images [1-5]. However, they seem not to be effective for practical accuracy inspection of the electro-mechanical systems because of its calculation time or adopted method itself. The techniques are roughly classified to three methods. The first method reconstructs the cross-sectional image based on the iterative calculation such as an expectation maximization (EM) method or an algebraic reconstruction technique (ART) [1-2]. The method requires a huge calculation power and it is difficult to apply the method to general CT devices because of the calculation time required for the imaging.

The second method is reported in visualization for guidance of cryosurgery [3]. Cryosurgery is a therapeutic procedure to ablate tissue by freezing injury. Proposed method in this report uses two CT images: one is scanned before the cryoprobes are inserted, and the other is scanned again after the cryoprobes are put in place. It is difficult to apply the method to non-destructive inspection.

The third method corrects x-ray projection data at where x-ray transmits high density materials [4-5]. The method localizes the metallic objects in the original CT image using a simple thresholding of CT numbers in the first procedure. Next, the extracted image of the metallic objects is provided for the forward projection to obtain ideal absorption by the objects. Then actual projection data is refined using the forward projected data. Although the method provides a significant improvement in image quality, there is a room for argument in the first procedure. That is, the original CT image with metal artifacts is insufficient to obtain accurate shapes and orientations of the metallic objects.

In this paper, we propose two CT reconstruction algorithms to reduce metal artifacts. Our methods basically stand on the third method and improve the method to solve the above mentioned problem from two approaches.

2. Materials and Methods

In this section, we describe investigations about the cause of the metal artifact. Then, we present detail procedures of our two methods.

2. 1 Investigation of a Cause of the Metal Artifact

Cross-sectional CT images are generally reconstructed from x-ray projections of the object at multiple angles [6-7]. The conventional CT reconstruction algorithm is based on the coherent x-ray absorption by the object. That is, when we radiate x-ray to a rotating object as illustrated in Fig. 1(a), the total amount of x-ray absorption measured by the x-ray detectors should be constant. However, there are significant variations in the total x-ray absorption depending on the radiating direction as shown in Fig. 1(c). The conventional reconstruction algorithm using such projection data produces a cross-sectional image with heavy metal artifacts as shown in Fig. 2.
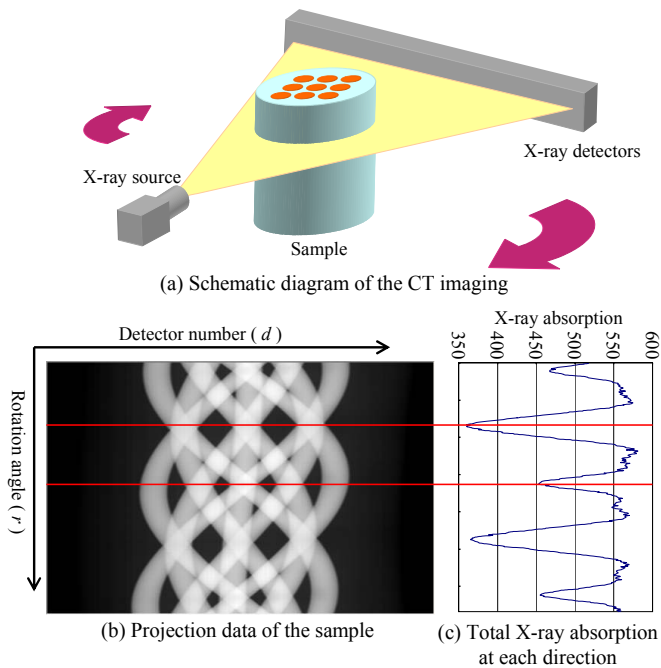
(a) Schematic diagram of the CT imaging

(b) Projection data of the sample

(c) Total X-ray absorption at each direction

Fig. 1 Experimentally measured projection data of a sample with nine steel shafts.
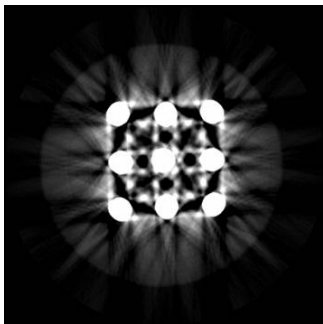
Fig. 2 Reconstructed image of the sample.

Fig. 3 Relationship between thickness of the metallic object and x-ray attenuation.

(a) Original image

(b) Reconstructed image using a calculated projection data

(c) Reconstructed image using a modified projection data
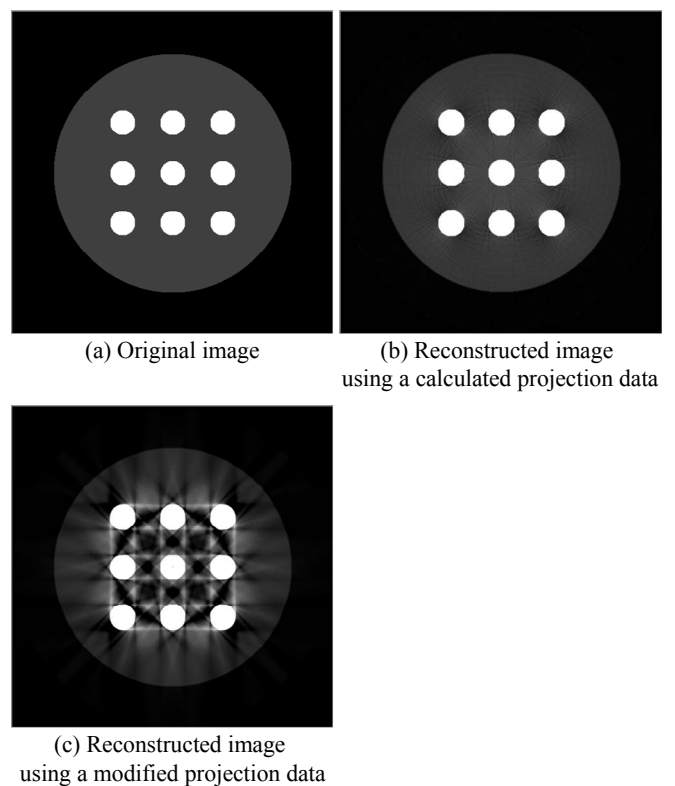
Fig. 4 Numerical analysis of the metal artifact.

In order to solve the problem, we have to investigate the characteristics of x-ray absorption by materials. Hence, we measured the relationship between thickness of metallic object and x-ray absorption. Measuring conditions in the experiment is as follows; the tube voltage on the x-ray source = 100kV, the tube current = 3μA. For a homogeneous absorber of attenuation coefficient μ, the experimental measurement of logarithm of a ratio of the number of photons that enter the object (N_{in}) to the number of photons that exit the object (N_{exit}) should be linearly proportional to the absorber thickness under ideal conditions. However, the measurement indicates nonlinear relationship as shown in Fig. 3. This suggests that there is inconsistent x-ray absorption in the practical scanning. We focus on the inconsistence of x-ray absorption, and perform the numerical simulation to examine effect on reconstructed images as following steps;

step 1. Formulation of the measured x-ray absorption.

step 2. Creation of a numerical cross-sectional image of a sample.

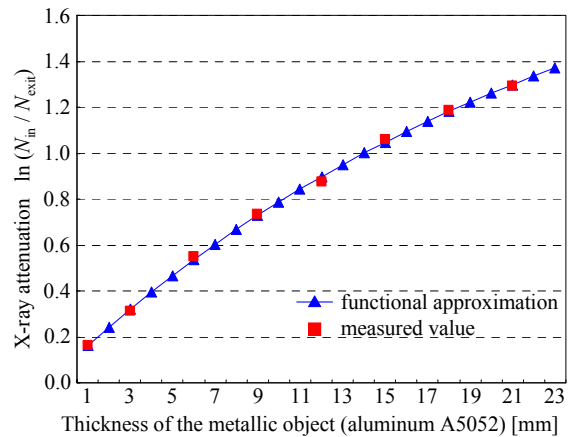step 3. Performing a numerical forward projection to the image.

step 4. Modifying the projection data according to the formulation.

Figure 4(a) shows the numerical cross-sectional image and Fig. 4(b) presents reconstructed image using the projection data computed in the step 3. They are almost same and the reconstruction with ideal projection data duplicates the image quite well. On the other hand, Fig. 4(c) shows a reconstructed image using the modified projection data in the step 4. The image has quite similar artifacts to the actual CT image shown in Fig. 2. That is, we confirm that nonlinearity of the x-ray absorption induces metal artifact in x-ray CT images.
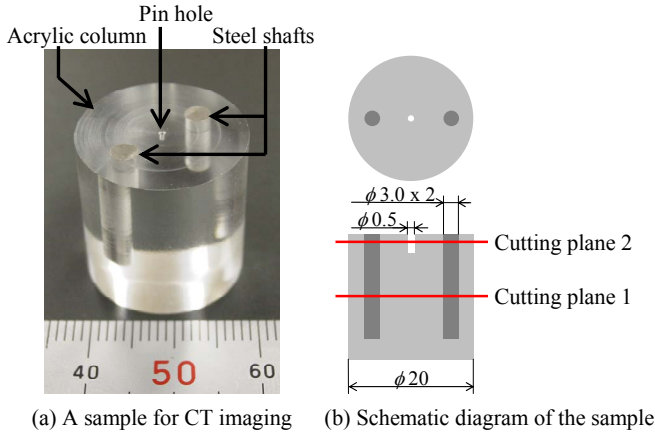
(a) A sample for CT imaging   (b) Schematic diagram of the sample

Fig. 5 Sample for explaining our methods.

2. 2 Method A: Direct Signal Conversion of a Projection Data

Our first method proposing in this paper extracts projection data corresponding to metallic objects and replaces the data to consistent values. This method is composed of the following five steps;

Step A1. Rough extraction of metal regions from the projection data.

Step A2. Determination of the metal regions.

Step A3. Computation of the cross-sectional shapes of the metallic objects.

Step A4. Calculation of the numerical projection data of the metal shape.

Step A5. Synthesis of measured and numerical projection data.

Detail description of the method is described as follows using a sample as shown in Fig. 5. The sample consists of an acrylic column and two steel shafts. The sample is provided to the CT scanning with following condition; the tube voltage on the x-ray source = 80kV, the tube current = 3μA. Figure 6(a) shows projection data at the cutting plane 1 indicated in Fig. 5(b). Figure 6(b) plots the profile of the x-ray attenuation at rotation angle r = 90 degrees of this projection data.

Step A1: Rough extraction of metal regions: We firstly extract the region where x-ray transmits high density materials from the projection data using a threshold. The threshold value is determined from a histogram of the x-ray absorption. The histogram of this example is shown in Fig. 7. The large frequencies at the attenuation values lower than 0.8 mean x-ray transmissions of air or an acrylic resin part. On the other hand, there are also large frequencies at the attenuation value about 2.5. They indicate x-ray transmissions of metallic objects. That is, the threshold between 1.0 and 2.0 separates metallic objects and others. In this case, we set 1.5 in the threshold and we modify the x-ray attenuation to 0.0 where the value is larger than the threshold as shown in Fig. 8(a).

Step A2: Determination of the metal region: The extracted data in the step A1 still remains transitional regions which depend on the threshold value. Then, we discriminate the regions using derivative values of the projection data. We adopt following two derivatives in consideration of measurement noises;
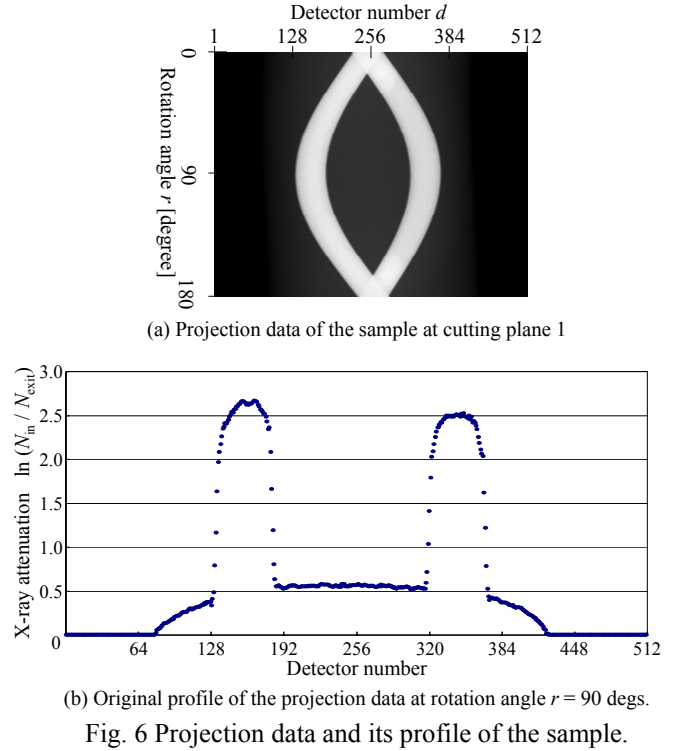

(a) Projection data of the sample at cutting plane 1

(b) Original profile of the projection data at rotation angle r = 90 degs.

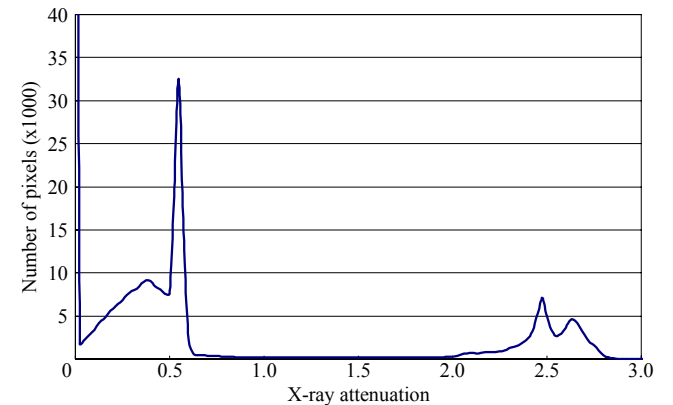Fig. 6 Projection data and its profile of the sample.

Fig. 7 Histogram of the X-ray attenuation.

$$D_1 = |f(d+1, r) - f(d, r)|, \qquad (1)$$
$$D_2 = |f(d+1, r) - f(d-1, r)|. \qquad (2)$$

Here, $f(d, r)$ is projection data at x-ray detector number d and rotation angle r. We determine the metal regions with larger D_1 and D_2 than each average value. The result in this step is shown in Fig. 8(b).

Step A3: Computation of the cross-sectional shapes: The modified projection data in the step A1 and A2 is provided to back projection and a cross-sectional image is computed. As the metal regions in the projection data was set to zero in the previous steps, the pixel corresponding to metallic objects also indicates zero in the image. So, we can easily extract shapes and locations of the metallic objects in the image. Figure 9(a) shows obtained image in this step and Fig. 9(b) shows extracted shapes of metallic objects from the image.
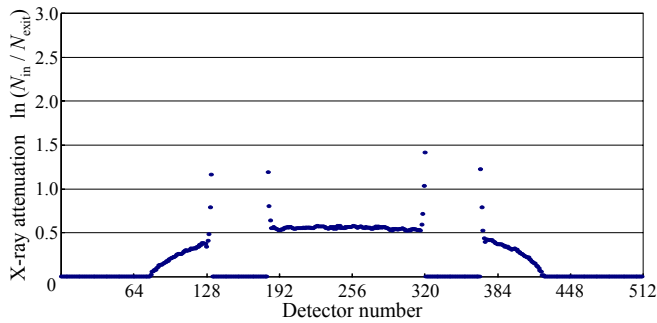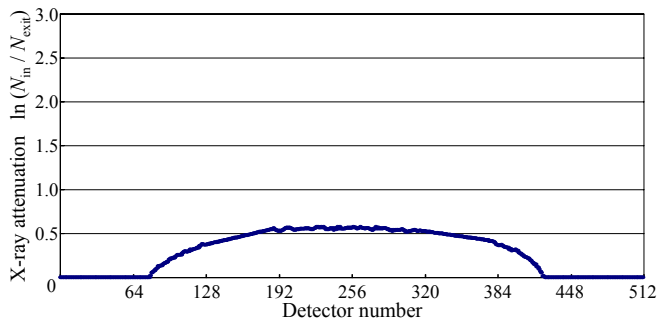
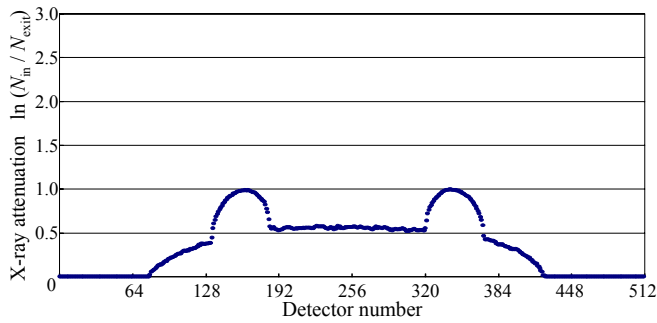(a) Modified projection data in the step A1.
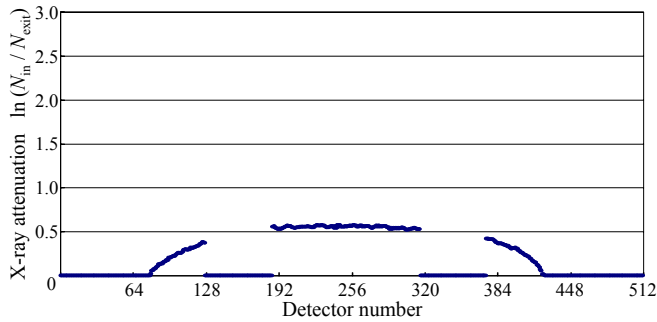
(b) Modified projection data in the step A2.
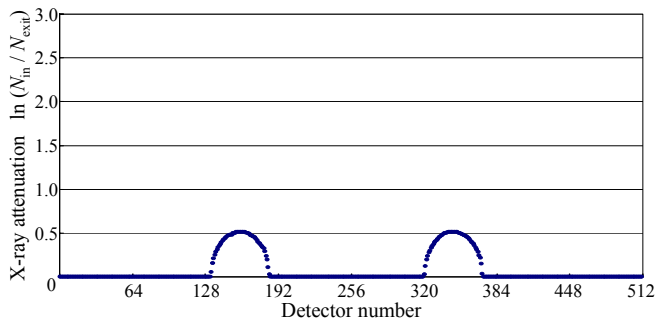
(c) Computed forward projection data of the metal objects in the step A4.
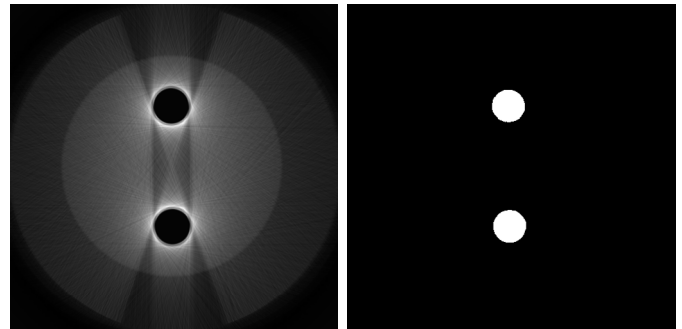

(d) Interpolated projection data in the step A5 (resin region).

(e) Combined projection data.

Fig. 8 Modification of the projection data in Method A.

(a) CT image without steel shafts   (b) Extracted shape of the shafts

Fig. 9 Cross-sectional image of the metallic object computed in the step A3.

Step A4: Calculation of the numerical projection data: Forward projection is applied to the computed image of the shapes of the metallic objects obtained in the step A3. This is equivalent to numerical x-ray radiation to the metallic objects. In the forward projection, we can configure lower x-ray attenuation coefficient μ to the metal region. In order to adjust x-ray attenuation by the metal region to the value which is comparable in magnitude to it by the resin region, we set $\mu = 0.01$ as the attenuation coefficient of the metallic object in this study. Figure 8(c) shows forward projection data.

Step A5: Synthesis of measured and numerical data: This step synthesizes the projection data modified in the step A1~A2 and the computed projection data in the step A4. Firstly, the metal regions in the modified projection data are linear interpolated as shown in Fig. 8(d). Then, computed projection data are added up to the data. Figure 8(e) shows rectified projection data. As this projection data indicate almost ideal attenuation, the data are anticipated to reconstruct a cross-sectional image without metal artifacts. The reconstructed image is shown in section 3.

2. 3 Method B: Use of Two Projection Data

Our second reconstruction method in this paper uses two projection data based on different x-ray intensities. The x-ray sources used for general CT devices do not produce monoenergetic x-ray photons but polychromatic ones including various wave lengths. There is a common phenomenon called beam hardening that high density materials relatively attenuate x-rays generated by low voltage x-ray tube compared with x-rays from high voltage tube. That is, a spectrum of the x-ray from a polychromatic source depends on the x-ray tube voltage and x-ray attenuation coefficient μ of the material is a function of the photon energy. Hence, the low energy photons to be preferentially absorbed by the object, so that the remaining beam becomes richer in high energy photons. This phenomenon of beam hardening prominently appears in high density materials. This tendency increases depending on the nonlinearity of x-ray attenuation. Our method utilizes the effect of beam hardening and corrects the projection data at which x-ray transmits high density materials. The method consists of following three steps;
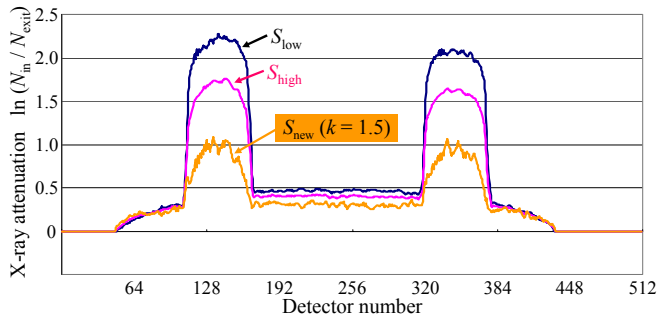
Fig. 10 Mathematical operation with two projection data.

Step B1. CT scanning with x-ray from low voltage tube and obtaining projection data S_{low}.

Step B2. CT scanning with x-ray from high voltage tube and obtaining projection data S_{high}.

Step B3. Mathematical operation with above two projection data.

Figure 10 shows the two projection data S_{low} and S_{high} of the object shown in Fig. 5. CT scanning of the sample is performed under following conditions; S_{low}: 80kV, 6μA and S_{high}: 130kV, 6μA. We can see that there are few differences at resin parts while there are large differences at metal parts. This means that we can coordinate the projection data of metal parts to the appropriate value using the two projection data. We perform a mathematical operation with the projection data S_{high} and S_{low}, and compute combined projection data S_{new} by the following equation.

$$S_{new} = (k+1)\,S_{high} - k\,S_{low} \qquad (3)$$

This equation provides consistent attenuation S_{new} at the resin region with equivalent value in S_{low} and S_{high} by the equation. On the other hand, S_{new} at the metal region is computed to the difference of S_{low} and S_{high} adjusted by the coefficient k. In this study, we empirically select the coefficient k.

3. Results and Discussions

In this section, we apply the proposed two reconstruction methods to several samples and discuss the efficiencies of the methods. Firstly, we show reconstructed images of the sample shown in Fig. 5. The conventional method reconstructs the image of the sample at the cutting plane 2 as shown in Fig. 11(b). The image has serious metal artifacts around the metallic objects and it is difficult to inspect the region between two shafts. Figures 11(c) is the image based on the proposed method A. The image by the method A has no artifacts and clearly represents a pin hole placed at the center of the sample. The result suggests that the method is quite efficient to inspect the void in the object with a simple structure. The method B reconstructs the image with the coefficient $k = 1.5$ as shown in Fig. 11(d). Although the method largely reduces artifacts, the central region of the sample is almost hidden by the remained artifact and the image is insufficient to observe the pin hole.

Secondly, the methods are applied to the sample with nine steel shafts in an acrylic column. In this case, the method A reduces the artifacts but the shapes of the metallic objects are deformed to the polygonal shapes as shown in Fig. 12(c). On the other hand, the reconstructed image as in Fig. 12(d) by the method B has weak artifacts but it presents exact metallic
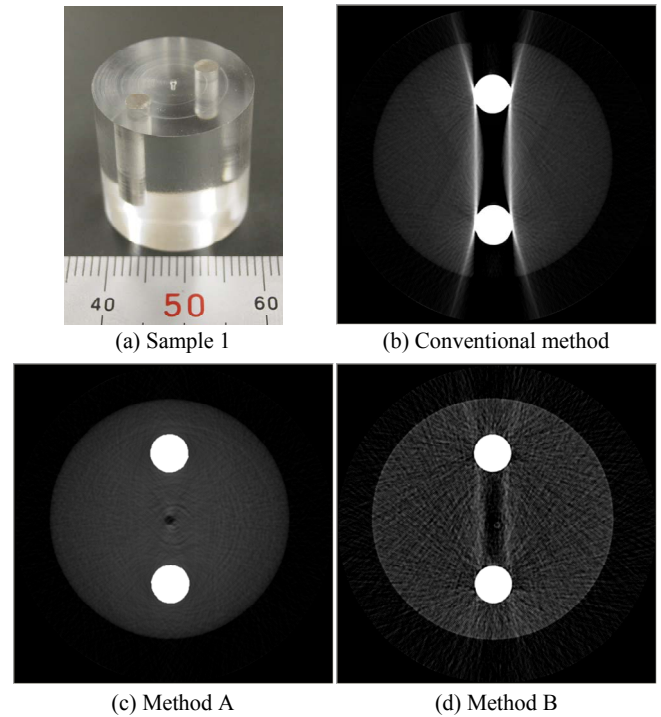

(a) Sample 1   (b) Conventional method

(c) Method A   (d) Method B

Fig. 11 Reconstructed images of the sample with two steel shafts in an acrylic column.

(a) Sample 2   (b) Conventional method
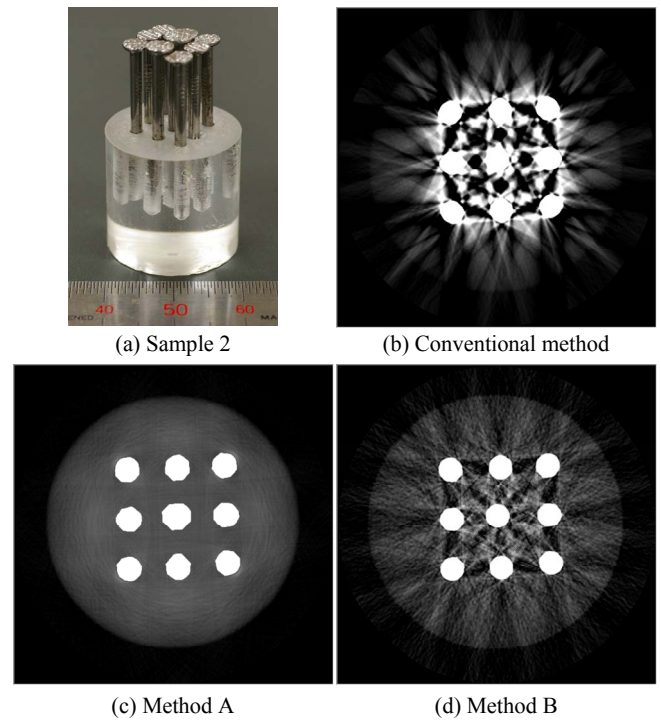
(c) Method A   (d) Method B

Fig. 12 Reconstructed images of the sample with nine steel shafts in an acrylic column.

shapes providing clear shape of the resin part sufficiently when the coefficient k is set to 1.2

Finally, we present the reconstructed images of the acrylic plate with a steel shaft in Fig. 13. The figure of resin plate is largely deformed in the reconstructed image by the method A. The method B reconstructs almost appropriate image of the whole sample with the coefficient $k = 1.5$.
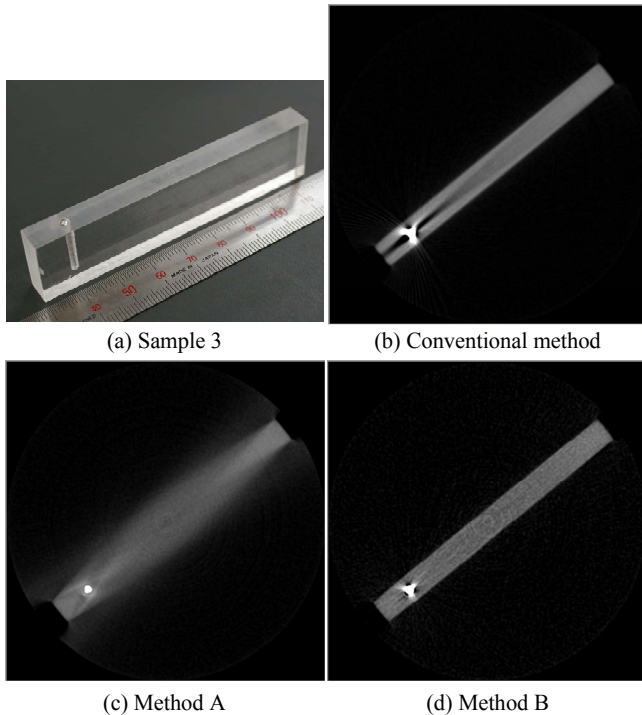
2006 Electronics Packaging Technology Conference

(a) Sample 3   (b) Conventional method

(c) Method A   (d) Method B

Fig. 13 Reconstructed images of the sample with a steel shaft in an acrylic plate.

These results suggest following findings;

Method A: it has a great efficiency to reduce metal artifacts from CT images. However, the shapes of metallic objects in the sample may be deformed by the method. In addition, it may reconstruct a quite invalid image depending on the structure of the sample.

Method B: it extracts appropriate shapes of not only the metallic objects but also the whole sample. However, the reconstructed image generally contains a lot of random noises and remains a few artifacts.

These findings mean that the method A has an advantage of the metal artifact reduction compared with the method B. As the method A performs numerical forward projection to the cross-sectional image of the metallic objects, the method corrects nonlinearity of the x-ray absorption appropriately. In contrast, although the efficiency of the method B depends largely on the setting of the coefficient k in equ. (3), the method is generally insufficient in terms of the correction of the nonlinearity.

On the other hand, we can see that the accuracy of the shape extraction by the method A is lower than that by the method B from above findings. This is caused by that the method uses simple thresholdings and converts the x-ray attenuation to 0.0 at the step A1 and A2 in the procedure of the method A.

Therefore, the advanced method integrating the two methods A and B is expected to achieve more accurate cross-sectional images. That is, combination of the shape extraction in the method B and forward projection in the method A will have great efficiency in the accuracy of the reconstructed images. Our further study will solve the above mentioned problems.

4. Conclusions

In this study, we aim to establish a non-destructive inspection technique of electro-mechanical systems using x-ray CT imaging. We examined the cause of the metal artifacts in the x-ray CT images and proposed two reconstruction methods to reduce them. The first method is a based on the direct signal conversion technique of the projection data, and the second method uses two projection data based on different x-ray intensities. We applied the methods to several samples and revealed the efficiency of the methods. Although each method has advantages and disadvantages, these methods supplement the disadvantage points each other and the advanced method composed of the two methods is expected to achieve more accurate cross-sectional images.

References

1. Wang, G., Snyder, D. L., O'Sullivan, J. A. and Vannier, M. W., "Iterative Deblurring for CT Metal Artifact Reduction," *IEEE Transactions on Medical Imaging*, Vol.15, No.5, (1996), pp.657–664.
2. Yokoi, T., "Image Reconstruction using Ordered Subsets-Expectation Maximization (OSEM) Algorithm," *Japanese Journal of Radiological Technology*, Vol.57, No.5, (2001), pp.523–529.
3. Wei, J., Sandison, G. A., Chen, L., Liang, Y. and Xu, L. X., "X-ray CT high-density artefact suppression in cryosurgery," *Physics in Medicine and Biology*, Vol.47, (2002), pp.N319–N326.
4. Tuy, H. K., "A Post-processing Algorithm to Reduce Metallic Clip Artifacts in CT images," *European Radiology*, Vol.3, (1993), pp.129–134.
5. Arai, Y. and Suzuki, M., Japanese patent, Publication number: 2001–190550.
6. Hounsfield, G. N., "Computed Medical Imaging, Nobel Lectures," *Physiology or Medicine 1971–1980*, (1992), pp.568–586, World Scientific Publishing Co.
7. Kak, A. C. and Slaney M., Principles of Computerized Tomographic Imaging, IEEE Press (New York, 1988).